Enhancement of Radiation-Resistant Effect in Ethylene–Vinyl Acetate Copolymers by the Formation of Ethylene–Vinyl Acetate Copolymers/Clay Nanocomposites

Wei-An Zhang,[1,2] Yue-E Fang[2]

[1]*Department of Polymer Science and Engineering, Shanghai Jiao Tong University, 800 Dongchuan Road, Shanghai 200240, China*
[2]*Department of Polymer Science and Engineering, University of Science and Technology of China, Hefei, Anhul 230026, China*

Received 19 July 2004; accepted 20 February 2005
DOI 10.1002/app.22299
Published online in Wiley InterScience (www.interscience.wiley.com).

ABSTRACT: Ethylene–vinyl acetate (EVA) copolymers/clay nanocomposites, prepared by using nonreactive organophilic clay and reactive organophilic clay, were characterized by X-ray diffraction and by high-resolution transmission electron microscopy. The influence of gamma irradiation on the structure and properties of the pure EVA and EVA/clay nanocomposites was systematically investigated. In the presence of gamma radiation, the clay can effectively restrain the increase of the storage modulus of EVA/clay nanocomposites, which was supported by dynamical mechanical analysis. Gamma irradiation had almost no effect on the thermal properties of EVA/clay nanocomposites by using nonreactive organophilic clay, but it obviously improved the thermal stability of EVA/clay nanocomposites by using reactive organophilic clay. © 2005 Wiley Periodicals, Inc. J Appl Polym Sci 98: 2532–2538, 2005

Key words: EVA; radiation; nanocomposites; clay; thermal properties

INTRODUCTION

Polymers are susceptible to deterioration during their use, especially in the presence of UV light or gamma irradiation. Many useful properties of polymers suffer gradual loss until, ultimately, the polymers become useless. In general, to retain the original good properties for a very long time, many methods were adopted such as blending stabilizers and coating the surface of the polymer. By these methods, the deterioration of the polymers can be slowed down to only a certain degree, although some other properties of the polymers may be damaged.

In recent years, polymer/clay nanocomposites have gained substantial interest in many research fields.[1–4] Compared with the pure polymer and microcomposites, polymer/clay nanocomposites can exhibit enhanced mechanical,[5,6] thermal,[7–9] and barrier[10,11] properties. Many previous studies have focused on these properties because these nanocomposites have great promise in such applications as coating, flame–retarding, barrier, and electronics materials. There are only a few works published on the new properties of these nanocomposites such as environmental stability.[12,13] EVA is a copolymer of ethylene and vinyl acetate and is widely used in many fields such as coating, shoeing, and telecommunication cable. In the past several years, the preparation methods and thermal and mechanical properties of EVA/clay nanocomposites have been widely studied.[14–16]

Like other polymers, EVA is also susceptible to crosslinking and main-chain scission during long-term use. In the study reported in this article we selected two different organclays to prepare EVA/clay nanocomposites. We mainly studied the effects of gamma radiation on the morphology and the properties of the two kinds of EVA/clay nanocomposites.

EXPERIMENTAL

Materials

EVA copolymer, containing 28 wt % vinyl acetate (VA), was supplied by Bayer AG (Leverkusen, Germany). Pristine sodium montmorillonite (Na-MMT), with a cation exchange capacity (CEC) value of about 100 mmol/100 g (Ling An Chemicals Co. Ltd., Hangzhou, China), was used as received. 2-(Dimethylamino) ethyl methacrylate, hexadecyltrimethylammonium bromide (HAB), 1-bromohexadecane, and ethyl acetate were all purchased from Shanghai Chemical Reagents Co. (China).

Correspondence to: W.-A. Zhang (wazhang@sjtu.edu.cn).

© 2005 Wiley Periodicals, Inc.

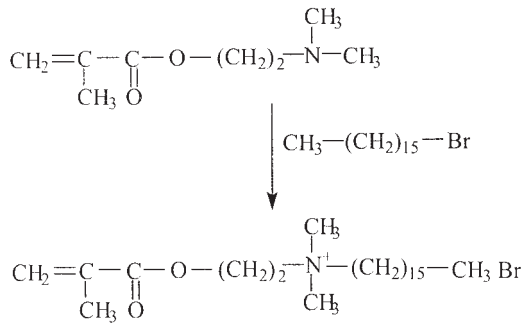

Scheme 1 Synthesis of the reactive intercalating agent MHAB.

Preparation of reactive clay-modifying agents for clay

The reactive clay-modifying agent 2-methacryloyloxyethylhexadecyldimethylammonium bromide (MHAB) was synthesized by the quaternization reaction as shown in Scheme 1.[17] 2-(Dimethylamino) ethyl methacrylate and 1-bromohexadecane (2:1 molar ratio) were reacted at 30°C for 24 h, in the presence of 3000 ppm inhibitor hydroquinone monomethyl ether. The product is insoluble and thus precipitates. The white powderlike precipitant was purified by filtering and by washing with ethyl acetate, after which it was dried under vacuum at ambient temperature for 24 h.

Preparation of organophilic clay

The organophilic montmorillonite (OMMT) was prepared through cationic exchange between Na-MMT and a clay-modifying agent in an aqueous solution. The suspension solution, containing 12.5 g of Na-MMT and 4.6 g of HAB, was mixed in 240 mL of distilled water. The suspension solution was stirred at room temperature for 24 h, after which the exchanged Na-MMT was filtered and washed with distilled water for several times until no bromide ion was detected with 0.1M $AgNO_3$ solution. Then the product was dried in a vacuum oven at room temperature for 24 h. The obtained OMMT was ground with a mortar and sieved by a Cu griddle with 280 mesh. This OMMT was denoted as HOM. By the same preparation method, the other OMMT, denoted as DHOM, was prepared from the exchange of 12.5 g of Na-MMT with 5.8 g of MHAB.

Preparation of EVA/clay nanocomposites

The EVA was first mixed with the 10 wt % OMMT in a rubber mill at 120°C and 32 rpm for 3 min, and another 10 min at 64 rpm. After mixing, the samples were hot-pressed for 3 min at 140°C under 10 MPa to form layers of suitable thickness. The size and thickness of the layers depend on the testing methods used in the present study.

Irradiation

EVA/OMMT nanocomposites samples were irradiated at room temperature in a vessel under atmospheric oxygen, with the 2.22×10^{15} Bq ^{60}Co γ-ray source. The dose rate was 65 Gy/min, and the range of dose was from 25 to 250 kGy. The irradiation doses were measured by a ferrous sulfate dosimeter.

Characterization

X-ray diffraction patterns were obtained by using a D/max γ X-ray diffractometer (XRD; Rigaku Denki, Tokyo, Japan), equipped with graphite monochromatized Cu–K_α radiation (λ = 0.154178 nm). The scanning range was 1.5–10° at a scanning rate of 2°/min.

The microstructure of nanocomposites was imaged using a 2010 EX high-resolution transmission electron microscope (HRTEM, JEOL, Tokyo, Japan). The samples for HRTEM were cut to 60 nm thick sections with a diamond knife.

Dynamic mechanical analysis (DMA) was carried out on a DMTA IV instrument (Rheometric Scientific, Piscataway, NJ) at a frequency of 1 Hz and heating rate of 2°C/min, from −50 to 80°C, at which the sample lost its dimensional stability.

The gel fraction was measured by extraction in boiling xylene for 72 h using a Soxhlet extractor, until the sample attained a constant weight. The gel fraction was calculated by the equation: gel fraction = $(w_2 - w_0)/(w_1 - w_0)$, where w_1 is the initial weight of the sample, w_2 is the weight of the insoluble portion, and w_0 is the weight of organoclay in the sample.

RESULTS AND DISCUSSION

Characterization of the structure of EVA/clay composites

Figure 1 shows the wide-angle X-ray diffraction curves of Na-MMT, HOM, EVA/HOM nanocomposites, and irradiated EVA/HOM nanocomposites. The basal spacing of the pristine Na-MMT was 1.33 nm, calculated from the peak position using the Bragg equation. After Na-MMT was modified with the HAB, its broad diffraction peak was shifted to a new peak at 4.45° (d = 1.98 nm), corresponding to the diffraction peak of HOM, which indicates that the organic quaternary ammonium salt has intercalated between the layers of the clay and increased the basal spacing of the clay. The weak peak for EVA/HOM nanocomposites indicates that the order of clay sheets was disturbed and seems partially exfoliated. Although EVA contains 28 wt % VA, this VA content is not enough to

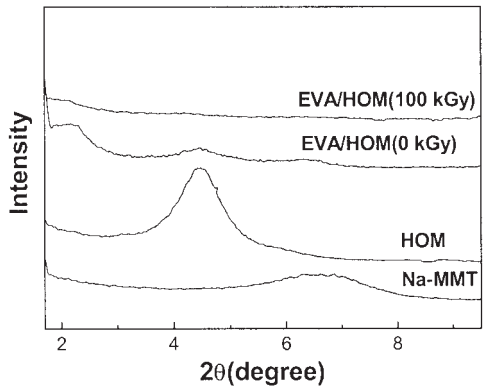

Figure 1 X-ray diffraction of Na-MMT, HOM, EVA/HOM nanocomposites, and EVA/HOM nanocomposites irradiated with 100 kGy.

confer to the EVA chains good flexibility and polarity to interact with HOM. Moreover, the basal spacing of the HOM is too narrow. Thus, by melt-blending, only some of the chains of EVA were wedged between the clay layers and thus the orderly structure of HOM was damaged. When the temperature becomes low, some chains perhaps move out from the clay layers because the chains of EVA crystallize. Thus, the XRD pattern of EVA/HOM verifies only that the orderly structure of clay layers was disturbed; in fact, the clay layers did not have adequate interaction with the EVA chains.

The structure of these nanocomposites, designated "wedged" nanocomposites, can be conformed by its HRTEM [see Fig. 3(a) below]. There is a big tactoid in this image, which is composed of many disordered layers of the clay. We clarified this structure in our previous study.[18] When EVA/HOM was irradiated with 100 kGy, part of the EVA28 chains began to degrade and crosslink. Then the peak of irradiated EVA/HOM became much broader because movement of the EVA chains further damaged the order of clay layers.

Figure 2 illustrates XRD patterns of DHOM, EVA/DHOM nanocomposites, and irradiated EVA/DHOM nanocomposites. The diffraction peak of DHOM is at 2.54° (d = 3.47 nm). The basal spacing of the DHOM is wider than that of HOM because the modified-clay agent contains another larger substituent.

The diffraction peak of EVA/DHOM nanocomposites is much more intense than that of EVA/HOM nanocomposites and the periodicity of diffraction is also clearer because the clay layers are still parallel to each other. These nanocomposites are thus called intercalated nanocomposites with respect to their structure. Because the spacing of the DHOM is much wider than that of HOM, the EVA28 chains are easily dispersed between the clay layers, and then the clay layers are well dispersed in these nanocomposites. This structure also appeared in its HRTEM [Fig. 3(b)]. We find that the XRD pattern of EVA/DHOM nanocomposites irradiated with 100 kGy is identical to that of nonirradiated EVA/DHOM nanocomposites, implying there is almost no effect of gamma radiation on the morphology of EVA/DHOM nanocomposites. Because the clay layers have a good dispersion in these nanocomposites, the clay layers can effectively decrease the degree of degradation and crosslinking and restrict the movement of the EVA chains.

Dynamic mechanical analysis of EVA/clay composites

Figure 4 illustrates the dynamic storage modulus (E') as a function of the temperature for pure EVA, EVA/HOM nanocomposites, and EVA/DHOM nanocomposites before and after irradiation. For the pure EVA [Fig. 4(a)], its dynamic storage modulus at 100 kGy is slightly lower than that of the nonirradiated sample below its glass-transition temperature (T_g). Then at around its T_g, the E' is almost the same as that of the nonirradiated sample. When the temperature is further increased, between −14 and 50°C, the E' is again lower than that of the nonirradiated sample.

This same trend of dynamic storage modulus also occurs for the EVA/HOM nanocomposites at 100 kGy [Fig. 4(b)], a phenomenon that likely occurs because EVA undergoes mainly main-chain rupture despite the low dose. The influence of oxygen is very important in the course of radiolytic reactions. Many polymers of the crosslinking type, such as polyethylene,[19] polypropylene,[20] and polystyrene,[21] undergo mainly main-chain rupture in oxygen or air even at low doses. Although there is no tetrasubstituted carbon in the backbone of EVA, it still can undergo main-chain rupture, which results from the oxygen brought into the EVA matrix during melt-blending and irradiation. For EVA/DHOM nanocomposites [Fig. 4(c)], however, the double bonds in the intercalating agent of DHOM can react with the broken chains of EVA under radi-

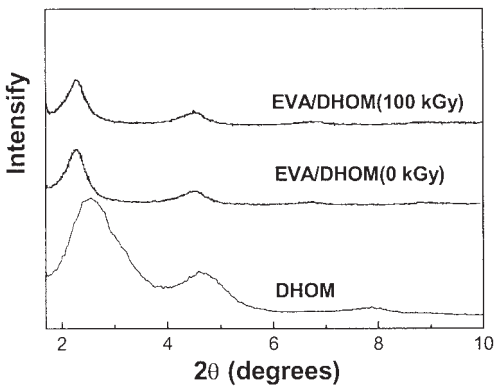

Figure 2 X-ray diffraction of DHOM, EVA/DHOM nanocomposites, and EVA/DHOM nanocomposites irradiated with 100 kGy.

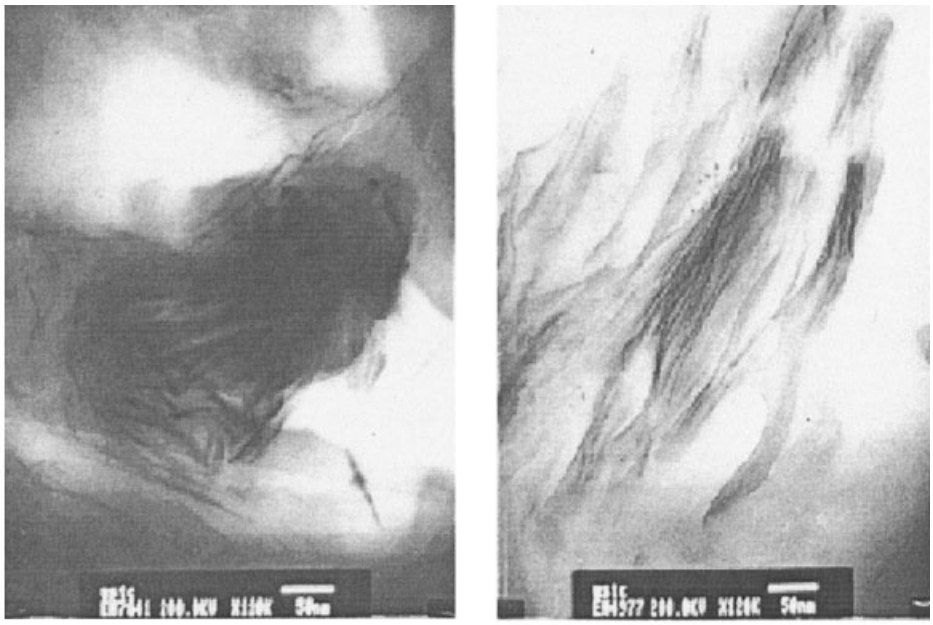

(a) (b)

Figure 3 HRTEM of EVA/clay nanocomposites (at ×120,000, 50-nm scale): (a) EVA/HOM nanocomposites; (b) EVA/DHOM nanocomposites.

ation and the reaction can make up for the decrease of its E' stemming from the main-chain rupture in the air. This is the reason that the E' of EVA/DHOM nanocomposites irradiated at 100 kGy is slightly higher than that of the nonirradiated samples.

When the radiation dose further increases to 200 kGy, the E' of the pure EVA is obviously higher than that of the nonirradiated sample and that of the irradiated at 100 kGy at the range of experimental temperature [Fig. 4(a)] because the crosslinking reaction becomes predominant. However, it is surprising to us that the E' of the EVA/HOM nanocomposites is still slightly lower than that of the nonirradiated samples below their T_g values at this dose, and that it becomes slightly higher than that of the nonirradiated sample only at temperatures beyond −15°C [Fig. 4(b)], possibly because the layers of HOM can absorb a large amount of radiation dose. These orderly layers of the clay are like shields, which effectively protect the chains of EVA from being irradiated. This phenomenon also occurs for EVA28/DHOM nanocomposites. The E' of EVA/DHOM nanocomposites irradiated by 200 kGy is slightly higher than that of nanocomposites irradiated by 100 kGy below their T_g values [Fig. 4(c)]. This is also because the clay layers are well dispersed in the nanocomposites and can absorb a large amount of radiation dose. Thus, the clay layers can effectively prevent the chains from crosslinking.

The loss tangent (tan δ) of pure EVA, EVA/HOM nanocomposites, and EVA/DHOM nanocomposites before and after irradiation are shown in Figure 5. The peak of the tan δ curve corresponds to the main relaxation processes, and the temperature at the main relaxation is taken as T_g. When the sample is irradiated at 100 kGy, the T_g values of the pure EVA and EVA/HOM nanocomposites are almost the same as those of the nonirradiated samples [Fig. 5(a) and (b)]. This is also because there is only a partial degradation of EVA, which has almost no effects on the T_g values. When the dose is increased to 200 kGy, the T_g of the pure EVA obviously shifts toward higher temperatures. For the EVA/HOM nanocomposites, however, the T_g only slightly shifts to a higher temperature, indicating that the clay layers can effectively prevent the EVA chains from crosslinking. For EVA/DHOM nanocomposites [Fig. 5(c)], at 100 kGy, its T_g obviously shifts toward higher temperature because some chains were grafted onto the surface of the clay layers. The clay layers can effectively restrict the movement of the chains when the temperature increases. When the radiation dose was further increased to 200 kGy, the double bonds of the intercalating agent of the DHOM were exhausted. The T_g of EVA/DHOM nanocomposites at 200 kGy also only slightly shifted to higher temperature because the clay layers have good dispersion in the nanocomposites and the clay layers can protect the chains from being decomposed.

Gel fraction of EVA/clay nanocomposites

Figure 6 shows the gel fraction of pure EVA and EVA/clay nanocomposites with different contents of

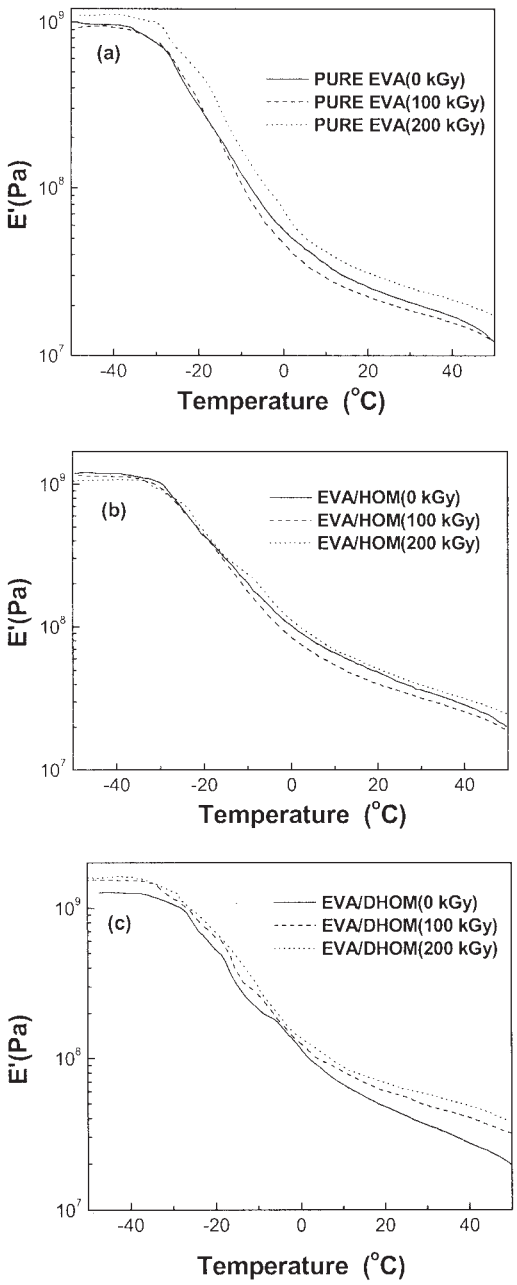

Figure 4 Storage modulus of pure EVA and EVA/clay nanocomposites with different doses: (a) pure EVA; (b) EVA/HOM nanocomposites; (c) EVA/DHOM nanocomposites.

HOM: 3 wt % (3HOM), 5 wt % (5HOM), and 10 wt % (10HOM). It can be seen that, as expected, the gel fraction increases with increasing radiation doses. It was surprising to us that the higher the content of HOM is, the more slowly the gel forms. When the dose is 25 kGy, a 55% gel formed for pure EVA, but only about 31% gel formed for the EVA/HOM nanocomposites with 10 wt % HOM because HOM protects the EVA chains from decomposition.

The sol fraction (s) of a radiation crosslinked polymer can be correlated to the inverse of the irradiation dose following the Charlesby–Pinner equation[22]:

$$s + s^{1/2} = p_0/q_0 + 10/(q_0UD)$$

where U is the number-average degree of polymerization, p_0 is the fracture density per unit dose (kGy^{-1}), q_0 is the density of crosslinked units per unit dose (kGy^{-1}), and D is the radiation dose (kGy). According

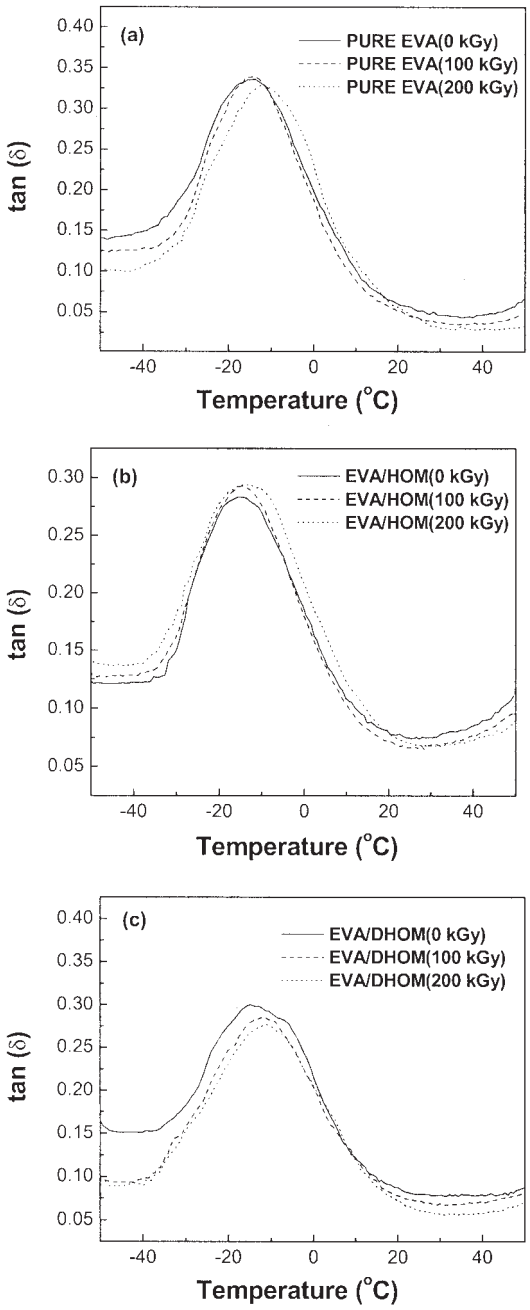

Figure 5 Tan δ of pure EVA and EVA/clay nanocomposites irradiated with different doses: (a) pure EVA; (b) EVA/HOM nanocomposites; (c) EVA/DHOM nanocomposites.

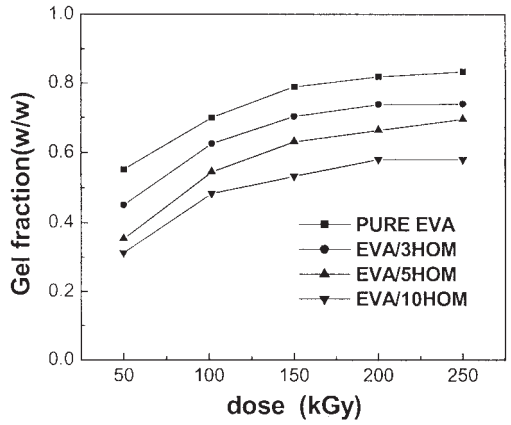

Figure 6 Gel fraction versus the radiation dose for pure EVA and EVA/HOM nanocomposites with different amounts of HOM.

to the Charlesby–Pinner equation, there is a linear correlation between $(s + s^{1/2})$ and $1/D$ (Fig. 7). This equation can be used to quantificationally predict the variation of the sol fraction according to the radiation dose to which EVA/clay nanocomposites are exposed.

Thermal gravimetric analysis of EVA/clay composites

The TGA thermograms of EVA/clay nanocomposites are shown in Figure 8. The thermal degradation temperature of EVA/clay nanocomposites undergoes two stages. The first is attributed to the elimination of acetate groups, which occurs between 310 and 400°C. The second is the main-chain degradation. At 100 kGy, we find that the onset decomposition temperature of the irradiated EVA/HOM nanocomposites is almost the same as that of the nonirradiated sample [Fig. 8(a)]. When the radiation dose increases to 200 kGy,

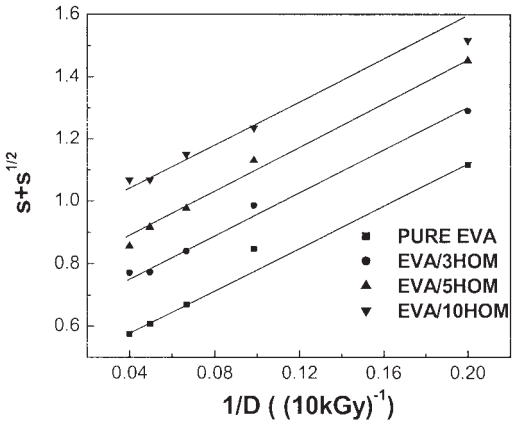

Figure 7 Plot of $\ln(s + s^{1/2})$ versus $\ln(1/D)$ for pure EVA and EVA/HOM nanocomposites with different amounts of HOM.

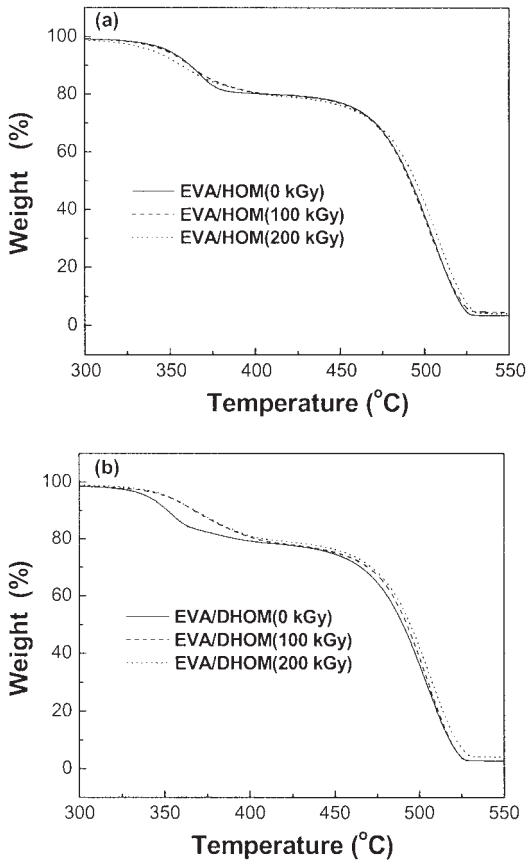

Figure 8 TGA thermograms of EVA/HOM nanocomposites and EVA/DHOM nanocomposites with different doses of radiation: (a) EVA/HOM and (b) EVA/DHOM nanocomposites.

however, the onset decomposition temperature of acetate groups becomes slightly lower. This perhaps occurs because more acetate groups were removed from the main chain with increasing dose, although the main chain is crosslinking. However, for EVA/DHOM nanocomposites, the onset decomposition degradation is obviously improved perhaps as a result of the reaction between the modifying-clay agents and the acetate groups, which effectively enhanced the thermal stability of the acetate groups [Fig. 8(b)]. Moreover, when the radiation dose was further increased, there is almost no increase for the decomposition temperature of acetate groups because the double bonds were exhausted. However, the decomposition temperature of the main chains is slightly increased, only because of the crosslinking reaction of main chains.

CONCLUSIONS

Under radiation, the orderly layers of clay in the EVA/HOM nanocomposites become much more disordered. For EVA/DHOM nanocomposites, however,

the structure is hardly affected by radiation. Compared to the storage modulus of the pure EVA and EVA/clay nanocomposites before and after irradiation, the crosslinking reaction of EVA/clay nanocomposites can effectively be prevented by clay. This is because the clay layers can absorb a large amount of radiation dose, as a shield protecting the EVA chains from being irradiated. Moreover, for EVA/DHOM nanocomposites, the thermal elimination temperature of acetate groups of EVA is obviously improved because the modified-clay agent can react with the EVA chains under radiation. Of course, the process may occur for other polymer/clay nanocomposites, when they are exposed to radiation such as UV light, gamma radiation, or electronic beams in air.

References

1. Usuki, A.; Kawasumi, M.; Kojima, Y.; Okada, A.; Kurauchi, T.; Kamigaito, O. J Mater Res 1993, 8, 1174.
2. Wang, Z.; Pinnavaia, T. J. Chem Mater 1998, 10, 3771.
3. Giannelis, E. P.; Krishnamoorti, R.; Manias, E. Adv Polym Sci 1999, 138, 107.
4. Matsumoto, A.; Oshita, S.; Fujioka, D. J Am Chem Soc 2002, 124, 13749.
5. Choi, Y. S.; Wang, K. H.; Xu, M. Z.; Chung, I. J. Chem Mater 2002, 14, 2936.
6. Maiti, P.; Yamada, K.; Okamoto, M.; Ueda, K.; Okamoto, K. Chem Mater 2002, 14, 4654.
7. Xie, W.; Xie, R. C.; Pan, W. P.; Hunter, D.; Koene, B.; Tan, L. S.; Vaia, R. Chem Mater 2002, 14, 4837.
8. Zhu, J.; Uhl, F. M.; Morgan, A. B.; Wilkie, C. A. Chem Mater 2001, 13, 4649.
9. Gilman, J. W. Appl Clay Sci 1999, 15, 31.
10. Fredrickson, G. H.; Bicerano, J. J. Chem Phys 1999, 110, 2181.
11. Nah, C. W.; Ryu, H. J.; Kim, W. D.; Choi, S. S. Polym Adv Technol 2002, 13, 649.
12. Yeh, J. M.; Liou, S. J.; Lai, C. Y.; Wu, P. C. Chem Mater 2001, 13, 1131.
13. Tidjani, A.; Wilkie, C. A. Polym Degrad Stab 2001, 74, 33.
14. Alexandre, M.; Beyer, G.; Henrist, C.; Cloots, R.; Rulmont, A.; Jerome, R.; Dubois, P. Macromol Rapid Commun 2001, 22, 643.
15. Li, X. C.; Ha, C. S., J Appl Polym Sci 2003, 87, 1901.
16. Jeon, C. H.; Ryu, S. H.; Chang, Y. W. Polym Int 2003, 52, 153.
17. Zeng, C. C.; Lee, L. J. Macromolecules 2001, 34, 4098.
18. Zhang, W. A.; Chen, D. Z.; Zhao, Q. B.; Fang, Y. E. Polymer 2003, 44, 7953.
19. Izumi, Y.; Nishii, M.; Seguchi, T.; Ema, K.; Yamamoto, T. Radiat Phys Chem 1991, 37, 213.
20. Ishigaki, I.; Yoshii, F. Radiat Phys Chem 1992, 39, 527.
21. Spiegelberg, S. H.; Cohen, R. E.; Argon, A. S. J Appl Polym Sci 1995, 58, 85.
22. Charlesby, A.; Pinner, S. H. Proc R Soc London 1959, A249, 367.